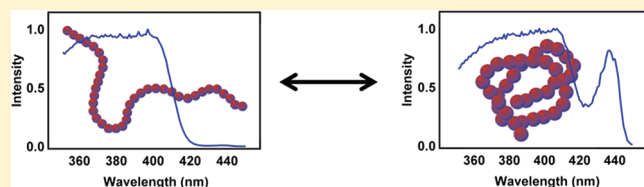


# Molecular Weight Effect on the formation of $\beta$ Phase Poly(9,9'-dioctylfluorene) in Dilute Solutions

Craig W. Cone, Ryan R. Cheng, Dmitrii E. Makarov, and David A. Vanden Bout\*

Department of Biochemistry and Chemistry, University of Texas at Austin, Austin, Texas 78712, United States

**ABSTRACT:** The effect of molecular weight on the formation of  $\beta$  phase poly(9,9'-dioctylfluorene) (PF8) was studied in dilute solutions. Temperature-dependent fluorescence experiments of unique synthetic batches as well as size-excluded single batches of polyfluorene were studied. Each batch had unique molecular weight, tetrahedral defect concentration, and polydispersity index (PDI). Polyfluorene was found to exhibit a temperature-dependent transition between two phases with distinct electronic transition signatures: the  $\alpha$  (primary) phase and the  $\beta$  (secondary) phase. In dilute solutions, the temperature at which the polymer exhibited a conversion between these phases showed a clear dependence on molecular weight. We model this transition temperature for  $\beta$  phase formation using the mean field theory for the coil–globule transition developed by Isaac Sanchez. Results show that temperature affects the average end-to-end distance corresponding to increases in secondary electronic absorption and that the dependence on temperature related to the coil–globule transition.



## INTRODUCTION

Organic semiconducting materials offer great potential as a new electronic material due to the ability to chemically tailor their properties through synthesis. In addition, organic materials, polymeric materials in particular, have demonstrated properties that can also vary strongly with morphology.<sup>1–3</sup> An excellent example of this is polyfluorene (PF), which is a polymerized blue emitting dye with a high quantum yield, and as such it is the basis for an entire class of organic electronic materials.<sup>4–8</sup> Such materials have been synthetically altered by copolymerization to modulate the conjugated electronic backbone or the addition of soluble side chains to tune the material properties to specific usages. Morphologically, polyfluorene presents two distinct phases in both films and solution. The  $\alpha$  phase of polyfluorene is the most common phase, achieved when the polymer is well solvated and in a random coil shape.<sup>9–11</sup> The secondary phase of polyfluorene is referred to as the  $\beta$  phase and has been reported to offer improved electronic properties.<sup>11–15</sup> As the  $\beta$  phase exhibits a lower energy excited state, the structure is believed to have adopted a planar zigzag structure with an extended conjugation length.<sup>16–20</sup> This new phase of PF was first reported by Grell et al. as the onset of lower-energy absorption and narrowed emission in pure poly(9,9'-dioctylfluorene) (PF8) and PF8 dispersed in polystyrene.<sup>21–23</sup> There have been many other ways in which the  $\beta$  phase of polyfluorene has been observed experimentally, such as varying the concentration and temperature, using poor solvents, thermal and vapor annealing, high boiling point solvents as solution additives, and nanofibers formed from porous alumina network templates.<sup>13,16,24–26</sup> Recently, it has been shown that at low temperatures ( $\sim 4$  K) the oligomer and long-chain polymers have similar emission characteristics.<sup>27</sup>

While there have been many studies of this secondary phase both in films and in solution, the mechanism of formation is still poorly understood.<sup>18</sup> Predominately it has been assigned to planarization of the backbone that is driven by side chain interactions in thin films of aggregates in solution.<sup>20,28</sup> However,  $\beta$  phase formation in dilute polymer solutions has been also demonstrated by Dias et al.<sup>29</sup> Similar to Dias we find that dilute PF8 formation of the  $\beta$  phase depends on intramolecular interactions. Previously, it has been shown that the temperature dependence of the  $\beta$  phase formation in dilute solution depends on the solvent quality.<sup>30</sup> This suggests that for dilute chains in solution  $\beta$  phase formation may be related to the interchain interactions that result from the collapse of the polymer rather than aggregation of multiple chains. While more concentrated studies have shown a complicated dependence on the length and connectivity of hydrocarbon side chains as well as solvent,<sup>29</sup> we contend that when dilute it is the collapse of the polymer from a freely solvated configuration to coil–globule that allows the side chain/side chain interactions to increase and drives the formation of the  $\beta$  phase. This paper will examine how molecular weight affects the formation of the  $\beta$  phase and correlate those changes with the effect molecular weight has on polymer collapse.

Polymer collapse can generally be understood through the concept of good and bad solvents. When a polymer chain is in good solvent, it expands into coil conformations to maximize solvent–monomer interactions. However, when a polymer chain is in bad solvent, it collapses into a globule conformation because

**Received:** June 28, 2011

**Revised:** September 6, 2011

**Published:** September 07, 2011

monomer–monomer interactions are more favorable. Changing the solvent quality from good to bad results in a collapse of a polymer chain from a swollen coil to a collapsed globule. The coil–globule transition can similarly be induced by a change in the temperature. At high temperatures, thermal fluctuations are strong enough to overcome intermonomer attraction, and so the polymer adopts coil conformations, which maximize its entropy. However, as temperature is decreased, the polymer adopts globule conformations because the favorable monomer–monomer interactions can no longer be overcome by thermal fluctuations.

While light-scattering techniques are typically employed to study polymer collapse directly, this is not possible with PF solutions as they rapidly aggregate upon cooling in all but very dilute solutions. However, it is possible to follow the formation of the  $\beta$  phase using absorption spectroscopy since the interconversion from  $\alpha$  to  $\beta$  phase is directly observable from the appearance of a new feature in the absorption spectrum at 437 nm associated with the  $\beta$  phase that occurs simultaneously with the decrease in the absorption spectral feature associated with the  $\alpha$  phase at 390 nm. Initially, in a good solvent the spectrum of a dilute PF8 will be free of  $\beta$  phase. If the temperature is lowered, the  $\beta$  phase peak will grow in. We quantify the amount of  $\beta$  phase formed as the percentage of primary absorption at 390 nm compared to the secondary absorption at 437 nm. The temperature dependence of the amount of  $\beta$  phase formed is characterized by a transition temperature,  $T_\beta$ , which corresponds to the point of greatest conversion between the phases. We estimate  $T_\beta$  by finding the inflection point in the temperature dependence of the amount of  $\beta$  phase, i.e.,  $d(\text{amount of } \beta \text{ phase})^2/d(\text{Temperature})^2|_{\text{Temperature}=T_\beta} = 0$ . Although the exact amount of conversion for each batch is dependent on molecular weight, defects, solvent, and other experimental variables,  $T_\beta$  is easily calculated from experimental data using finite difference. Furthermore,  $T_\beta$  can then be compared to the coil–globule transition temperature,  $T_{cg}$ , obtained numerically from Sanchez's theory.

## EXPERIMENTAL SECTION

For this research, four unique synthetic batches of poly(9,9'-dioctylfluorene) were utilized that had all been synthesized via a Suzuki coupling reaction.<sup>31</sup> The hexamer oligomer was purchased from American Dye Source and used without further purification. All batches were characterized using gel permeation chromatography (GPC) to determine the average molecular weight and polydispersity index (PDI). Shorter conjugation length has been shown that there is a shorter wavelength absorption maximum.<sup>32</sup> Tetrahedral defects were estimated using UV–vis where the number of defects is related to the length of the maximum energy absorption.

GPC was used to characterize individual polymer batches while also creating a physically separate distribution of molecular weights which were then collected into individual fractions and analyzed using temperature-dependent fluorescence measurements. The solvent was evaporated, and remaining size-excluded polymer was solvated in methyl-cyclohexane (MCH), which is a poor solvent with a low freezing point.

A modified SPEX Fluorolog 1 from Horiba Jobin Yvon with a 450 W xenon lamp was used for all temperature-dependent measurements. The instrumentation was controlled via a custom labview program. All excitation spectra were collected from 350 to 450 nm for emission at 475 nm.

For each measurement, a dilute sample was prepared (50  $\mu\text{L}$  of 1% by weight PF8 in MCH) in a standard rectangular quartz fluorescence cuvette with a screw top. The molecular weight separated samples were diluted to fill a 3 mL sample cuvette as the samples had been diluted substantially during GPC analysis. All samples measured had concentration less than  $10^{-3}\%$  PF8 by weight percent.

For each temperature-dependent fluorescent experiment, the solution was heated to remove all aggregated polymer species and cooled to room temperature. The sealed cuvette was placed in a Janis ST-100 optical cryostat, and a Lakeshore temperature controller was used to cool the cryostat to the desired temperature. Once the sample had reached the desired temperature, it was allowed to equilibrate for 15 min before optical measurements were collected. At low temperatures the experiments were limited by the formation of larger polymer aggregates which lead to high intensity spikes in the emission as well as visibly inhomogeneous samples. Every run was considered complete when large nonreversible aggregates were formed.

The temperature dependence of the  $\beta$  phase formation for each batch was probed by observing changes in the excitation spectra of the polymers in dilute solution. While the excitation spectra are not direct analogues to the absorption spectra, the experimentally observed results show only a slight difference. There is an increase in the amount of  $\beta$  phase compared to  $\alpha$  phase in the excitation spectra compared to the absorption spectra due to energy transfer. The effect is small; moreover, we are only looking at ratios of the  $\beta$  phase, so if the percentage calculated is systematically overestimating the percentage, then it is immaterial to the analysis. All samples were created highly dilute (50  $\mu\text{L}$  of 1 wt % PF8/MCH stock solution, with 3 mL of MCH added) for every experiment and were considered complete after the formation of large aggregates was observed in the emission spectra as detected by spikes in the fluorescence intensity. All samples analyzed exhibited this phenomena with the exception of PF8 batches D and E, in which the solvent freezing point was reached before the formation of large aggregates was spectroscopically detected.

**Theory of Coil–Globule Transition.** There have been many theoretical models describing the coil–globule transition in polymer chains.<sup>33</sup> Flory first approached the problem of polymer collapse by describing a polymer chain as a cloud of monomers contained within the volume occupied by the polymer chain where only binary interactions between monomers are taken into account.<sup>34</sup> Since then, works building upon Flory's theory have demonstrated the importance of higher-order intrachain interactions in properly describing the coil–globule transition as well as the globule conformations of a polymer.<sup>33,35</sup> Here we adopt the model due to Sanchez,<sup>35</sup> which (approximately) accounts for binary, tertiary, and all higher-order intrachain interaction terms unlike other models that only account for binary and tertiary interactions. Furthermore, Sanchez's model has been shown to provide a quantitative description of the coil–globule transition of polystyrene<sup>35,36</sup> and polypeptides.<sup>37</sup>

Sanchez's model, in particular, provides the temperature dependence of the swelling parameter,  $s = R_g/R_{g,0}$ , where  $R_g$  is the polymer's radius of gyration and  $R_{g,0}$  is the mean radius of gyration of the ideal chain. Specifically, this dependence is given by

$$\frac{7\phi_0}{3N}\left(\frac{1}{s^3} - \frac{1}{s}\right) = \frac{1}{2} \frac{\theta\phi_0^2}{Ts^6} + \ln\left(1 - \frac{\phi_0}{s^3}\right) + \frac{\phi_0}{s^3} \quad (1)$$

**Table 1.** Summary of the Physical Characteristics of the Different PF8 Batches

name	molecular weight (kDa)	polydispersity Index (PDI)	average monomer units
A	100000	2.56	216
B	76000	2.38	164
C	30000	2.5	65
D	6500	1.47	13
E	2500	1.00	5

where  $N$  is the degree of polymerization (i.e., chain length);  $\theta$  is the theta temperature for the polymer chain; and  $\phi_0$  is the monomer volume fraction of a polymer chain with a radius of gyration of  $R_{g,0}$ . For polymer chain consisting of  $N + 1$  monomers with a bond length of  $l_b$ ,  $R_{g,0}$  can further be written as  $R_{g,0} = l_k(n_k/6)^{1/2} = (Nl_k l_b/6)^{1/2}$ , where  $L = Nl_b$  is the contour length,  $l_k$  is the Kuhn length, and  $n_k = L/l_k$  is the number of Kuhn segments. Assuming that each monomer is a sphere of radius  $l_b$  and the polymer chain occupies a volume of radius  $R_{g,0}$ , the parameter  $\phi_0$  can then be written as  $\phi_0 = \Lambda/(4\pi R_{g,0}^3/3)$  where  $\Lambda = (4\pi l_b^3/3)(1 + 11N/16)$  represents the smallest volume that the polymer chain can occupy taking into account that consecutive beads are overlapping because the monomer radius is taken to be equal to the bond length. This expression simplifies to  $\phi_0 = (l_b/l_k)^{3/2}(1 + 11N/16)(N/6)^{-3/2}$ . Note that  $(l_b/l_k)^{3/2} \ll 1$  corresponds to stiff polymer chains, whereas  $(l_b/l_k)^{3/2} \sim 1$  corresponds to flexible chains. Here, we use a Kuhn length of  $l_k = 15$  nm and a bond length  $l_b = 0.836$  nm for PF8<sup>23</sup> such that  $(l_b/l_k)^{3/2} \approx 0.013$ .

**Estimation of  $T_{cg}/\theta$  from Theory.** As a polymer chain goes from a good solvent to a bad solvent (e.g., temperature is decreased), it undergoes a transition from a swollen coil to a collapsed globule. The temperature at which the attractive intrachain interactions are balanced by the entropy gain due to swelling is called the coil–globule transition temperature,  $T_{cg}$ . Sanchez derived an approximate expression for  $T_{cg}$  of the form

$$N^{1/2} \left( \frac{\theta - T_{cg}}{T_{cg}} \right) = \varphi \quad (2)$$

where  $\varphi$  is a positive constant that is dependent on the stiffness of the polymer chain and  $(\theta - T_{cg})/T_{cg}$  is the normalized width of the transition, which scales with chain length as  $(\theta - T_{cg})/T_{cg} \sim N^{-1/2}$ . In the limit of infinite chain length, the width of the transition approaches zero, and eq 2 leads to the expected result of  $T_{cg} = \theta$ . At this temperature, one has  $s = 1$  so that the polymer size is equal to that of the ideal chain. However, for chains of a finite length, the transition temperature is below the theta point, i.e.,  $T_{cg} < \theta$ , and the transition width broadens with decreasing chain length.

Here, we numerically compute the dependence of the swelling parameter  $s$  on  $T/\theta$  (using eq 1) for different values of the chain length  $N$ . In general,  $s$  monotonically increases with increasing  $T/\theta$  from the globule state (i.e.,  $T/\theta \ll 1$ ) to the coil state (i.e.,  $T/\theta > 1$ ). For stiff polymer chains such as PF8 ( $(l_b/l_k)^{3/2} \ll 1$ ), we find that Sanchez's theory predicts a discontinuous jump in the swelling parameter where  $T_{cg}/\theta$  is estimated as the point of discontinuity. The value of  $T_{cg}/\theta$  where this happens was described using the Sanchez equation (eq 2).

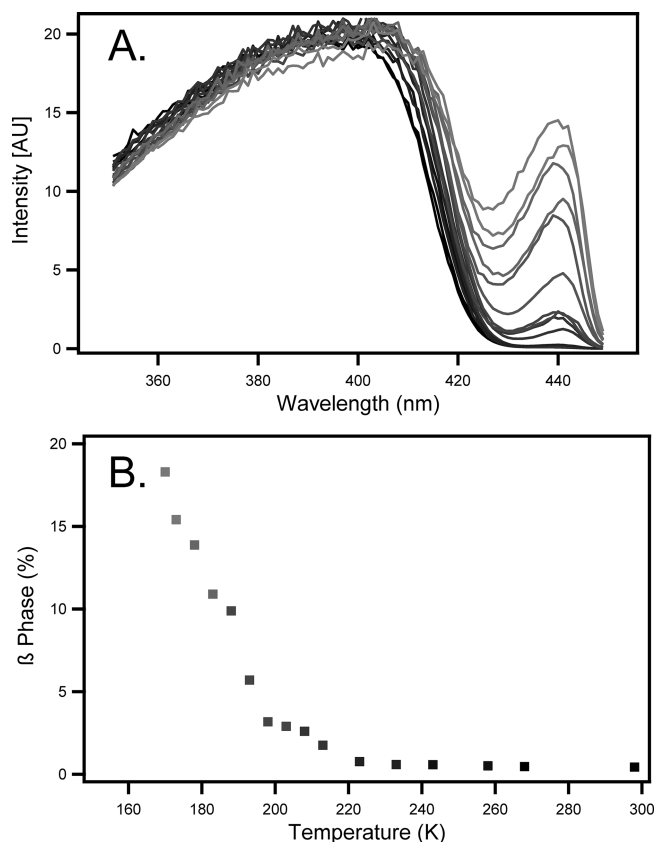


**Figure 1.** (A) Excitation spectra as a function of temperature of a dilute solution of PF8 in MCH. The chemical structure of polyfluorene is shown in the inset. (B) The calculated % of the  $\beta$  phase is shown for each temperature.

**Estimation of  $\theta$  for PF8.** The constant  $\varphi$  can be estimated as  $\varphi \approx 3.55$  by fitting the numerically obtained dependence of  $T_{cg}/\theta$  on  $N$  to eq 2. Assuming that the  $\beta$  phase transition is described by the coil–globule transition (i.e.,  $T_\beta = T_{cg}$ ) where  $\varphi \approx 3.55$ , one can then use eq 2 to fit the experimental data for the dependence of  $T_\beta$  on  $N$ . This fit results in an estimate of the  $\theta$  temperature for PF8 ( $\theta \approx 311.9$  K), while the quality of this fit provides a direct measure of the validity of mean field coil–globule transition theory in application to our experimental data.

## RESULTS AND DISCUSSION

Standard polymer characterizations were performed using GPC to determine the average molecular weight and polydispersity index (PDI) for each PF8 batch used. Table 1 shows the summary of the experimentally determined physical properties. Average molecular weight ranged from 6.5 to 100 kDa (16 to 225 repeat units), and every PDI value was above 2.0 except the exceedingly low molecular weight polymer. For clarity: A refers to the largest polymer, D to the smallest polymer, and Batch E to the oligomer sample which never shows secondary phase absorption under any conditions. Suzuki coupling polymerizations are known to have a large polydispersity index (PDI) and be susceptible to tetrahedral defect creation along the conjugated backbone of the repeated unit.<sup>38</sup>

The presence of a  $\beta$  phase can be detected by the formation of a new absorption band at 437 nm. Excitation spectra are recorded for dilute solution rather than absorbance spectra in more concentrated solutions to avoid interchain aggregation.



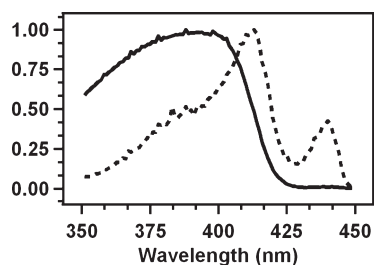


**Figure 2.** The two most important spectral features, which were extracted from a single series of sample measurements using singular value decomposition. The solid line corresponds to the calculated  $\alpha$  phase absorption, while the dotted line corresponds to the calculated  $\beta$  phase absorption.

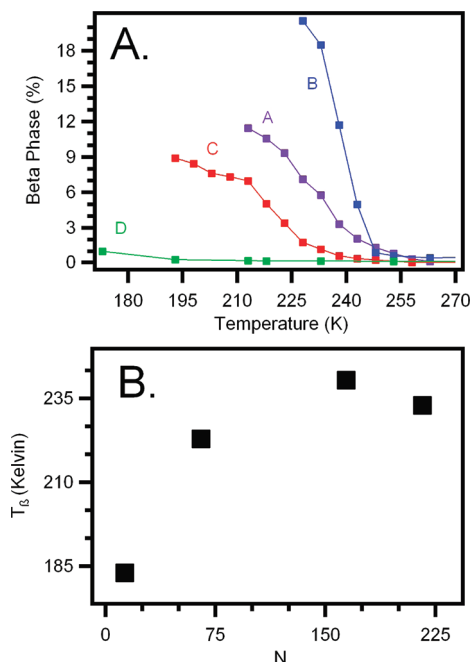


**Figure 3.** (A) Cooling curves for four different batches of polyfluorene as a function of  $\beta$  phase formation as the temperature is cooled. (B) Comparison of the results where the chain length,  $N$  (e.g., molecular weight), is compared to the measured transition temperature,  $T_\beta$ , observed in A.

The amount of  $\beta$  phase formed was estimated by the percentage of primary absorption at 390 nm compared to the secondary absorption at 437 nm. The onset, mid, and final temperatures are unique to each batch of PF. Figure 1A shows a typical increase in secondary absorption as a function of temperature. In Figure 1B the percentage of the  $\beta$  phase is plotted as the temperature decreased. The change in the spectrum as a function of temperature contains overlapping absorption, and singular value decomposition was used to quantify the change in absorption.

Singular value decomposition (SVD) is a numerical technique that provides the minimum number of spectral features required to completely represent data sets.<sup>39–41</sup> In this case, it was used to quantify the amount of  $\beta$  phase and spectral features associated with the  $\beta$  absorption. SVD was performed on the data set, and it was found that the two spectral species represent each polymer data set. Each experiment was treated

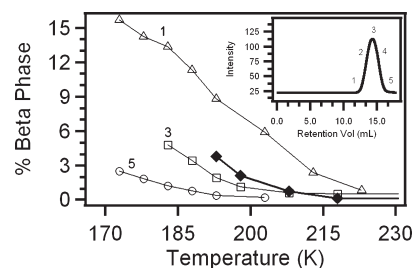


**Figure 4.** Temperature-dependent fluorescence results for polymer B. The bulk temperature-dependent fluorescence result is shown with  $\blacklozenge$ , while the results for the differing molecular weights are shown with open symbols. Inset shows gel permeation chromatography data from which molecular weight dependent samples were generated.

individually rather than combining all the data in one set due to defects in the  $\alpha$  phase and conjugation lengths. While SVD results vary with experiment, they yielded unique curvatures and maxima, and key results were conserved and not different in any substantive form. The SVD method allows for the extraction of the spectral features associated with  $\beta$  phase absorption. As Figure 2 shows, the spectral features extend beyond the most obvious peak at 437 nm. There is a vibronic progression of peaks which are similar to the results seen previously and were extracted using subtraction. The results from SVD can be compared to previous results reported by Chunwaschirasiri et al., who modeled the  $\beta$  phase optical properties as a more ordered conjugated backbone and performed quantum mechanical calculations which yielded satisfactory results when compared to the calculated excitation spectrum for the  $\beta$  phase.<sup>42</sup>

At each point along the experimental cooling curve, the percent of  $\beta$  phase does not change as a function of waiting time. Moreover, if the temperature is returned to a previous value, the percentage of the  $\beta$  phase is reproduced. This indicates the system is at equilibrium at every temperature measured. However, at lower temperatures macroscopic aggregates begin to form that disrupt the experiment irreversibly. Therefore, the lowest reported temperature is before the onset of aggregation formation. The absorbance maximum of the  $\beta$  phase is different, then the main absorption of PF8, but easily relatable to the transition temperature for  $\beta$  phase formation,  $T_\beta$ .

$T_\beta$  corresponds to the point of greatest conversion between the phases as estimated from the point of inflection, i.e.,  $d(\% \beta \text{ phase})^2/dT^2|_{T=T_\beta} = 0$ . This is trivial to estimate using finite difference methods from the experimental data as long as there are suitable data points and signal.  $T_\beta$  was calculated from experimental data for each batch of PF8 and is plotted as a function of degree of polymerization in Figure 3. The highest temperature is found for polymer B, but the largest molecular weight is found for polymer A. However, each synthetic batch of polymer has both a different molecular weight and defect concentration. Polymer A has the largest molecular weight but did not have the highest transition temperature or the largest amount of  $\beta$  phase formed. The number of defects in the different polymer batches can be estimated from the maximum of the primary  $\alpha$  absorption as the defects tend to break the extended conjugation and shift the absorption to higher energy. Polymer B has the least number of defects as judged from having the lowest-energy absorption. It also has the highest transition temperature and most  $\beta$  phase observed.

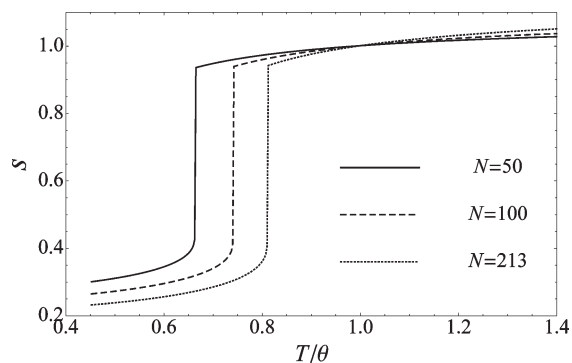


**Figure 5.** Swelling parameter computed numerically from eq 1 for varying polymer lengths demonstrates a transition from an expanded coil to a collapsed globule with decreasing  $T/\theta$ . These transitions were first order (discontinuous) with a normalized transition temperature of  $T_{cg}/\theta$  at the discontinuity, characteristic of stiff polymer chains.

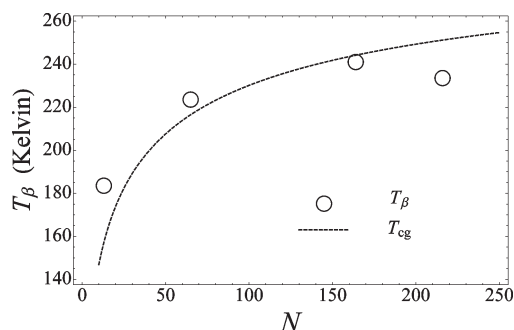


**Figure 6.** Chain length dependence of  $T_\beta$  plotted in comparison with  $T_{cg}$ .  $T_{cg}/\theta$  was rescaled by  $\theta \approx 311.9$  K, which was obtained from fitting  $T_\beta$  with eq 2. This fit suggests that in the limit of  $N \rightarrow \infty$   $T_{cg}$  converges to  $\theta \approx 311.9$  K.

To isolate the molecular weight effect on the formation of the  $\beta$  phase in PF8, a system containing a similar concentration of defects must be studied. A single batch of PF8 was physically separated using GPC. The concentration of tetrahedral defects along a conjugated backbone of PF8 should remain fairly uniform and should depend on the reaction conditions. Generally, it is polymer systems with large PDIs ( $x > 2.0$ ) that are poor systems; however, in this case they are extremely useful as it allows for large variation in the molecular weights of the sample collected after GPC analysis. The physical separation of polymers based on size was performed on PF8 batch A. Figure 4 shows the temperature dependence of percent  $\beta$  phase for three distinct fractions for polymer A. Three distinct fractions were created by collecting five separate aliquots and analyzing the largest, smallest, and intermediate samples (inset of Figure 4). Figure 4 also shows full batch data ( $\blacklozenge$ ). The highest molecular weight fraction has the highest  $T_\beta$ , and the lowest molecular weight fraction has the lowest  $T_\beta$ . The average fraction has a value of  $T_\beta$  similar to that of the ensemble average. This shows a clear dependence on the molecular weight of PF8 on the formation of  $\beta$  phase absorption in solution. Molecular weight dependence is subtle in contrast to the contribution of defects, which can dominate the trend. For the GPC fractionated portions of polymer B, all of the values of  $T_\beta$  are within the experimental noise. The results of the physical separation of a single polymer

batch show that the  $T_\beta$  of any polymer depends on the molecular weight such that decreasing the molecular weight results in a decrease in  $T_\beta$ . This agrees with the theoretically predicted trend for molecular weight dependence on the temperature of collapse of chains with finite length.

To examine the molecular weight dependence of chain collapse, we used Sanchez's theory for the coil–globule transition, as described in preceding sections. Representative dependences of the swelling parameter on  $T/\theta$ , as predicted by this theory for different values of chain length, are shown in Figure 5. The swelling coefficient increases monotonically with  $T/\theta$  and exhibited a first-order discontinuous transition located at  $T_{cg}/\theta$ . Such a transition is characteristic of a stiff polymer chain, i.e.,  $(l_b/l_k)^{3/2} \ll 1$ . A theta temperature was estimated for PF8 as  $\theta \approx 311.9$  K (see section Estimation of  $\theta$  for PF8 for details), allowing for a direct comparison of the chain length dependence for the transition temperature  $T_{cg}$ , as estimated from eq 2, with  $T_\beta$  (Figure 6). We find that the mean field coil–globule transition theory qualitatively agrees with the experimental data. This suggests that in the limit of infinite chain length  $T_\beta$  asymptotically approaches  $\theta \approx 311.9$  K with a narrowing normalized transition width,  $(\theta - T_\beta)/T_\beta$ , that scales with chain length as  $(\theta - T_\beta)/T_\beta \sim N^{-1/2}$ . However, it should be noted that in Figure 6  $N = 54$  corresponds to only  $\sim 3$  Kuhn segments. It is unclear if the dependence described by eq 2 yields meaningful information for such short chains. Nevertheless, the agreement between collapse of polymer and formation of the  $\beta$  phase in polyfluorene is very encouraging because it suggests a possible relationship between two previously unrelated phenomena. This relationship should be explored further.

In this report, we observe a secondary solution phase of polyfluorene in dilute solutions. The  $\beta$  phase was observed in dilute solutions of isolated polymer chains to avoid intermolecular interactions and isolate the intrachain interactions. Excitation measurements were taken at equilibrium so that a phase transition could be observed. Multiple batches with unique characteristics (average molecular weight, polydispersity index, and tetrahedral defect concentration) were measured. There is also a strong dependence on the length of the polymers and the total amount of  $\beta$  phase formed which is expected because longer polymers have a larger number of available conformations; however, this effect is not as pronounced as the dependence on defect concentration. As defect concentration helps to define the amount of  $\beta$  phase possible for any given batch of polyfluorene, the polymer with the lowest defect concentration shows the largest percentage of  $\beta$  phase formed.

The  $T_\beta$  in each experiment is the temperature where there is the greatest amount of interconversion between the  $\alpha$  and  $\beta$  phases. If the  $\beta$  phase arose only from a planarization of the polymer chain, the physical separation based on molecular weight results should all be within the experimental error because planarization is only a polymer–solvent interaction and does not depend on intrachain interactions. This is clearly not the case as the data show a trend that is dependent on molecular weight. This supports the idea that intrachain interactions are required to form the  $\beta$  phase for isolated chains of solution-phase polyfluorene.

## CONCLUSIONS

In conclusion,  $\beta$  phase formation in polyfluorene is dependent on many specific factors. While higher molecular weight can be related to higher transition temperatures, the defect concentration

determines the amount of  $\beta$  phase possible. The midpoint and  $T_\beta$  in each experiment is the point at which the energetics of polymer–polymer and polymer–solution are evenly balanced. If the  $\beta$  phase arose only from a planarization of the polymer chain, the physical separation based on molecular weight results should all be within the experimental error as planarization is only a polymer–solvent interaction and does not<sup>43</sup> alone cause collapse of the polymer from solution. We have also shown that simplistically using the mean field theory of the coil–globule transition developed by Sanchez leads to qualitative agreement with the experimental data, suggesting a possible connection with the coil–globule transition of a single polymer chain. Such a connection needs to be explored more thoroughly in future studies. Thus, in this paper we have shown the correlation between polymer collapse, defects, and the secondary phase of polyfluorene using temperature-dependent fluorescence measurements and the theory of the coil–globule transition.

## AUTHOR INFORMATION

### Corresponding Author

\*E-mail: davandenbout@mail.utexas.edu. Phone: (512) 232-2824.

## ACKNOWLEDGMENT

C.W.C. was supported by the Robert A. Welch Foundation (Grant F-1377 to D.A.V.). Welch summer scholar Abigail Wolf was of assistance with the portions of the experimental procedures. R.R.C. was supported by the Robert A. Welch Foundation (Grant F-1514 to D.E.M.). We would also like to thank Micah S. Glaz for helpful comments on the manuscript.

## REFERENCES

- Hu, D.; Yu, J.; Wong, K.; Bagchi, B.; Rossky, P. J.; Barbara, P. F. *Nature* **2000**, 405, 1030.
- Barbara, P. F.; Gesquiere, A. J.; Park, S.-J.; Lee, Y. J. *Acc. Chem. Res.* **2005**, 38, 602.
- Rozanski, L. J.; Cone, C. W.; Ostrowski, D. P.; Vanden Bout, D. A. *Macromolecules* **2007**, 40, 4524.
- Scherf, U.; List, E. J. W. *Adv. Mater.* **2002**, 14, 477.
- Sims, M.; et al. *J. Phys.: Condens. Matter* **2005**, 17, 6307.
- Zhu, B.; Han, Y.; Sun, M.; Bo, Z. *Macromolecules* **2007**, 40, 4494.
- Janietz, S.; Bradley, D. D. C.; Grell, M.; Giebeler, C.; Inbasekaran, M.; Woo, E. P. *Appl. Phys. Lett.* **1998**, 73, 2453.
- Weinfurter, K.-H.; Fujikawa, H.; Tokito, S.; Taga, Y. *Appl. Phys. Lett.* **2000**, 76, 2502.
- Leclerc, M. J. *Polym. Sci., Part A: Polym. Chem.* **2001**, 39, 2867.
- Kim, Y.; Vanden Bout, D. *Appl. Phys. A: Mater. Sci. Process.* **2009**, 95, 241.
- Klaerner, G.; Miller, R. D. *Macromolecules* **1998**, 31, 2007.
- Ryu, G.; et al. *J. Phys.: Condens. Matter* **2007**, 19, 056205.
- Da Como, E.; Becker, K.; Feldmann, J.; Lupton, J. M. *Nano Lett.* **2007**, 7, 2993.
- Prins, P.; Grozema, F. C.; Nehls, B. S.; Farrell, T.; Scherf, U.; Siebbeles, L. D. A. *Phys. Rev. B* **2006**, 74, 113203.
- Azuma, H.; Kobayashi, T.; Shim, Y.; Mamedov, N.; Naito, H. *Org. Electron.* **2007**, 8, 184.
- Tsoi, W. C.; Charas, A.; Cadby, A. J.; Khalil, G.; Adawi, A. M.; Iraqi, A.; Hunt, B.; Morgado, J.; Lidzey, D. G. *Adv. Funct. Mater.* **2008**, 18, 600.
- Kilina, S.; Batista, E. R.; Yang, P.; Tretiak, S.; Saxena, A.; Martin, R. L.; Smith, D. L. *ACS Nano* **2008**, 2, 1381.
- Peet, J.; Brocker, E.; Xu, Y.; Bazan, G. C. *Adv. Mater.* **2008**, 20, 1882.

- Caricato, A. P.; Anni, M.; Manera, M. G.; Martino, M.; Rella, R.; Romano, F.; Tunno, T.; Valerini, D. *Appl. Surf. Sci.* **2009**, 255, 9659.
- Bright, D. W.; Dias, F. B.; Galbrecht, F.; Scherf, U.; Monkman, A. P. *Adv. Funct. Mater.* **2009**, 19, 67.
- Grell, M.; Bradley, D. D. C.; Inbasekaran, M.; Woo, E. P. *Adv. Mater.* **1997**, 9, 798.
- Grell, M.; Bradley, D. D. C.; Inbasekaran, M.; Ungar, G.; Whitehead, K. S.; Woo, E. P. *Synth. Met.* **2000**, 111–112, 579.
- Grell, M.; Bradley, D. D. C.; Long, X.; Chamberlain, T.; Inbasekaran, M.; Woo, E. P.; Soliman, M. *Acta Polym.* **1998**, 49, 439.
- Cadby, A. J.; Lane, P. A.; Wohlgenannt, M.; An, C.; Vardeny, Z. V.; Bradley, D. D. C. *Synth. Met.* **2000**, 111, 515.
- Cheun, H.; Tanto, B.; Chunwaschirasiri, W.; Larson, B.; Winokur, M. J. *Appl. Phys. Lett.* **2004**, 84, 22.
- Caruso, M. E.; Anni, M. *Phys. Rev. B* **2007**, 76, 054207.
- Da Como, E.; Borys, N. J.; Stroehriegel, P.; Walter, M. J.; Lupton, J. M. *J. Am. Chem. Soc.* **2011**, 133, 3690.
- Bright, D. W.; Galbrecht, F.; Scherf, U.; Monkman, A. P. *Macromolecules* **2010**, 43, 7860.
- Dias, F. B.; Morgado, J.; Mañá, A. n. L.; da Costa, F. P.; Burrows, H. D.; Monkman, A. P. *Macromolecules* **2006**, 39, 5854.
- Kitts, C. C.; Vanden Bout, D. A. *Polymer* **2007**, 48, 2322.
- Miyaura, N.; Suzuki, A. *Chem. Rev.* **1995**, 95, 2457.
- Song, J.; Liang, W. Z.; Zhao, Y.; Yang, J. *Appl. Phys. Lett.* **2006**, 89, 071917.
- Grosberg, A. Y.; Khokhlov, A. R. *Statistical Physics of Macromolecules*; AIP Press: New York, 1994.
- Flory, P. J. *Principles of Polymer Chemistry*; Cornell University Press: New York, 1953.
- Sanchez, I. C. *Macromolecules* **1979**, 12, 980.
- Swislow, G.; Sun, S.-T.; Nishio, I.; Tanaka, T. *Phys. Rev. Lett.* **1980**, 44, 796.
- Sherman, E.; Haran, G. *Proc. Natl. Acad. Sci.* **2006**, 103, 11539.
- Brookins, R. N.; Schanze, K. S.; Reynolds, J. R. *Macromolecules* **2007**, 40, 3524.
- Shafer, M. W.; McKee, G. R.; Schlossberg, D. J. *Rev. Sci. Instrum.* **2008**, 79, 10F534/1.
- Zhao, Y.; Schmidt, M. J. *Appl. Crystallogr.* **2009**, 42, 734.
- Stamatopoulos, V. G.; Karras, D. A.; Mertzios, B. G. *Meas. Sci. Technol.* **2009**, 20, 104021/1.
- Chunwaschirasiri, W.; Tanto, B.; Huber, D. L.; Winokur, M. J. *Phys. Rev. Lett.* **2005**, 94, 107402.
- Mueller-Spath, S.; Soranno, A.; Hirschfeld, V.; Hofmann, H.; Rüegger, S.; Reymond, L.; Nettels, D.; Schuler, B. *Proc. Natl. Acad. Sci.* **2010**, 107, 14609.